

# Palaeoenvironmental evolution of the Barbate–Trafalgar coast (Cadiz) during the last ~140 ka: Climate, sea-level interactions and tectonics

Cari Zazo <sup>a,\*</sup>, Norbert Mercier <sup>b</sup>, Javier Lario <sup>c</sup>, Elvira Roquero <sup>d</sup>, José-Luis Goy <sup>e</sup>, Pablo G. Silva <sup>e</sup>, Ana Cabero <sup>a</sup>, Francisco Borja <sup>f</sup>, Cristino J. Dabrio <sup>g</sup>, Teresa Bardají <sup>h</sup>, Vicente Soler <sup>i</sup>, Ana García-Blázquez <sup>e</sup>, Luis de Luque <sup>a</sup>

<sup>a</sup> Departamento de Geología, Museo Nacional de Ciencias Naturales-CSIC, 28006-Madrid, Spain

<sup>b</sup> Laboratoire des Sciences du Climat et de l'Environnement, CEA-CNRS, Av. de la Terrasse, 91198 – Gif-Sur-Yvette Cedex, France

<sup>c</sup> Departamento de de Ciencias Analíticas, Facultad de Ciencias-Universidad Nacional de Educación a Distancia (UNED), 28040-Madrid, Spain

<sup>d</sup> Departamento de Edafología, ETS I. Agrónomos, Universidad Politécnica, 28040-Madrid, Spain

<sup>e</sup> Departamento de Geología, Facultad de Ciencias, Universidad, 37008-Salamanca, Spain

<sup>f</sup> Área de Geografía Física, Facultad de Humanidades, Universidad de Huelva, 21007 Huelva, Spain

<sup>g</sup> Departamento de Estratigrafía-UCM and Instituto de Geología Económica-CSIC, Universidad Complutense, 28040-Madrid, Spain

<sup>h</sup> Departamento de Geología, Universidad de Alcalá, 28871-Alcalá de Henare, Spain

<sup>i</sup> Estación Volcanológica de Canarias, Instituto de Productos Naturales-CSIC). Avenida Astrofísico Francisco Sánchez, 3. 38206-La Laguna, Tenerife, Spain

## ABSTRACT

Coastal response to tectonic activity and eustatic-climate interactions during the Late Pleistocene and Holocene has been analyzed along the Barbate–Trafalgar shoreline. The study area consists of an uplifted platform (La Breña, ~140 m) bounded by two major NW–SE faults that have created two subsiding areas: Meca in the west and Barbate in the east. The areas of subsidence have favoured the accumulation of a thick morphosedimentary sequence consisting of (in ascending stratigraphic order) beach, alluvial, and aeolian deposits, which repeatedly underwent soil-forming processes. This study outlines the palaeogeographical evolution of the area over the last ~140 ka, as deduced from geomorphological mapping associated with a range of laboratory analyses (mineralogical, geochemical, magnetic susceptibility, and soil micromorphology analyses), optically stimulated luminescence (OSL dating), and existing U–Th dating. Special attention has been paid to the alluvial unit, made up of vertically stacked sandy sheet-flood deposits with interbedded red paleosols. OSL ages suggest that sediment supply to the alluvial/coastal environments took place mainly at the end of the two most recent glacial periods (Oxygen Isotopic Stage [OIS] 6 and OIS 3/OIS 2) and during the last interglacial period (end of OIS 5). This means that although alluvial sedimentation took place at times of relatively high sea level, these were not times of highstand because very high sea levels (like the present) allow marine erosion of the distal part of the fans (fan toes), cutting cliffed coasts.

The repeated occurrence of paleosols in the alluvial sequence seems to indicate a recurrence of environmental changes that modified the feedback relationships between the catchment and the coastal areas. These changes are recorded in repeated oscillations of soil parameters, and are revealed from the results of geochemical and environmental magnetism analyses. We associate repeated pedogenesis and alluvial sedimentation with the glacial/interglacial global climatic changes due to an oscillating humidity/aridity ratio rather than with cyclicity in thermal regime.

## 1. Introduction

The sedimentary record of the evolving coastal sedimentary environments during the last interglacial–last glacial–present interglacial transitions is well exposed along several tracts of the coastal

cliffs of the Gulf of Cadiz, on the southern Spanish coast (Fig. 1). Outstanding examples are the Asperillo (Huelva Province) and Barbate–Meca (Cádiz Province) cliffs. However, despite the excellent outcrops, dating the dominantly-terrestrial deposits has proved to be very unreliable, thus hampering any precise interpretation of the relations between processes/morphologies and temporal evolution. A recent exception, however, is a paper by Zazo et al. (2005) that focuses on the Huelva coast and incorporates OSL data from terrestrial deposits.

The sequence of Quaternary deposits exposed along the cliffs between Barbate and Trafalgar Cape rests unconformably on Late Miocene deposits. Previous papers (Zazo, 1980; Zazo and Goy, 1990;

\* Corresponding author. Fax: +34 91 564 47 40.

E-mail addresses: mcncz65@mncn.csic.es (C. Zazo), mercier@lsce.cnrs-gif.fr (N. Mercier), Javier.Lario@ccia.uned.es (J. Lario), elvira.roquero@upm.es (E. Roquero), joselgoy@usal.es (J.-L. Goy), pgsilva@usal.es (P.G. Silva), acabero@mncn.csic.es (A. Cabero), fborja@uh.es (F. Borja), dabrio@geo.ucm.es (C.J. Dabrio), teresa.bardaji@uah.es (T. Bardaji), vsoler@ipna.csic.es (V. Soler), amgb78@usal.es (A. García-Blázquez), mcnl150@mncn.csic.es (L. Luque).



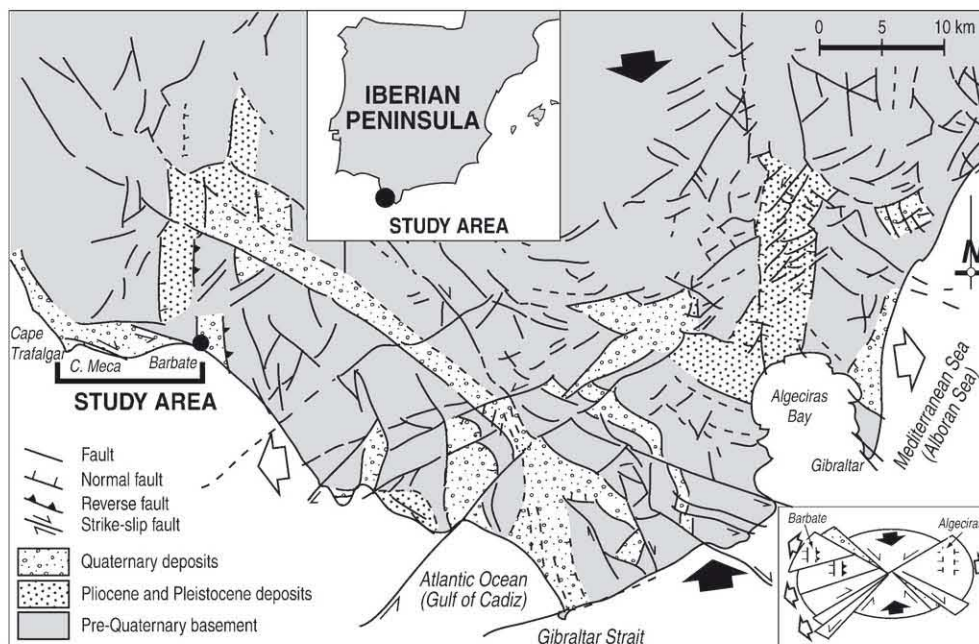


**Fig. 1.** Main structural features in the Spanish central sector of the Gibraltar Strait and kinematic model (stress diagram). Black arrows: orientation of the compressive stress field; white arrows: orientation of the subsidiary extension (simplified from Goy et al., 1995). C. Meca: Caños de Meca.

Borja, 1992) have distinguished three units in ascending order: beach deposits dated as last interglacial OIS 5c (Zazo et al., 1999); reddish sandy deposits including a few channel-shaped conglomeratic bodies, assigned to the Soltanian cycle (Würm); and aeolian dunes.

The study of ice cores (e.g. Dansgaard et al., 1993) and ocean sediments (e.g. Bond et al., 1993) revealed prominent millennial to sub-millennial atmospheric and oceanic climatic variability both during glacial and interglacial periods (McManus et al., 1999). Results from cores in the Atlantic Ocean at latitudes close to the Gulf of Cadiz and the Alboran Sea in the Western Mediterranean (Sánchez-Gómez et al., 1999; Cacho et al., 1999, 2002; Moreno et al., 2002; Sánchez-Gómez et al., 2002; Martrat et al., 2004) indicate a conspicuous sensitivity of these regions to record millennial climatic and oceanographic changes. The main indicators of these oscillations are the changes of surface sea-water temperatures (SST) and vegetation that occur in phase with the North Atlantic climatic variability. Indeed, cold events in Greenland (Heinrich, Dansgaard-Oeschger stadials) are reflected in southern Iberia as arid events with steppe vegetation, decreased river runoff, enhanced dust transport from the Sahara, and lower SST.

The aim of this paper is to contribute to a better understanding of the regional response of coastal environments to the tectonic, climatic, and eustatic changes during the last ~140 ka which are recorded in the sedimentary sequences exposed in the cliffs of the Barbate and Trafalgar Cape zone, a present-day tectonically active area. This study is enhanced by luminescence (OSL) dating techniques that, when combined with the limited U/Th data, allowed a tighter time control on the sedimentary sequence. Particular attention has been paid to the alluvial fan deposits with interbedded paleosols that separate the Last-interglacial beach deposits from a younger generation of aeolian dunes. These deposits provide vital information on the processes (erosion, accumulation, and pedogenesis) that took place during an interglacial-glacial climatic cycle.

## 2. Geological and physiographical framework

The study area is located at the south-eastern end of the Gulf of Cadiz (Fig. 1) at the western emerged termination of the Betic Cordillera. Here, the nappes of the Campo de Gibraltar Complex have

been squeezed between the approaching External and Internal Betic Zones since the early Tertiary (Benkhelil, 1976). Tectonics exert a primary control on the present morphology of the shoreline, particularly on the orientation of coastlines and the lower reaches of rivers. The recent tectonic pattern in the area is explained by pure shear kinematics (Goy et al., 1995) caused by the convergence of Africa and Eurasia: the orientations of the two largest, most prominent, tectonic lineations are NE-SW and NW-SE. The first has worked as a dextral strike-slip fault and the second as a sinistral strike-slip fault (Fig. 1, inset). The intersection of the two systems in the Strait of Gibraltar area created a central crustal block in the Strait zone and two lateral blocks: the Atlantic (to the west) and the Mediterranean (to the east), and promoted an extensional tectonic setting since at least the Pliocene (Benkhelil, 1976; Sanz de Galdeano and López Garrido, 1991; Goy et al., 1995). Connected to this pattern, two subsidiary distensive troughs with N-S orientations (Barbate and Algeciras Bay) were created in both lateral blocks, and became the main depocentres of Pliocene marine and fluvio-marine Pleistocene sedimentation.

The present elevation of the Quaternary marine terraces (Zazo et al., 1999) indicates a maximum uplift during the last ~130 ka in the central zone of the Strait of Gibraltar of approximately 19.5 m (OIS 5e marine terrace), the highest elevation ever measured in all the Iberian coasts. In contrast, lower elevations have been measured along the Atlantic (12–13 m) and Mediterranean (5–7 m) coasts, associated with the lateral blocks.

The coastal tract studied in this paper lies in the western border of the Barbate trough (Fig. 1) which affects the late Miocene biocalcarrenites. The trough had been filled during the Pliocene with yellow siliciclastic sands including a few fossiliferous layers indicative of upper shoreface, beach environments. These are topped by the non-fossiliferous “Red Sands”, interpreted as estuarine deposits indicative of the regional Plio-Pleistocene regression. It is believed that the Plio-Pleistocene deposits are closely related to the main water courses flowing into the Gulf of Cadiz, including the Barbate River (Fig. 2).

The climate in the area is of Mediterranean-Atlantic type, with mean annual rainfall around 550 mm/yr, mostly concentrated in winter months. Mean temperatures range between 16 and 19 °C, with a thermal amplitude of 10–16 °C. Prevailing winds blow from SW and



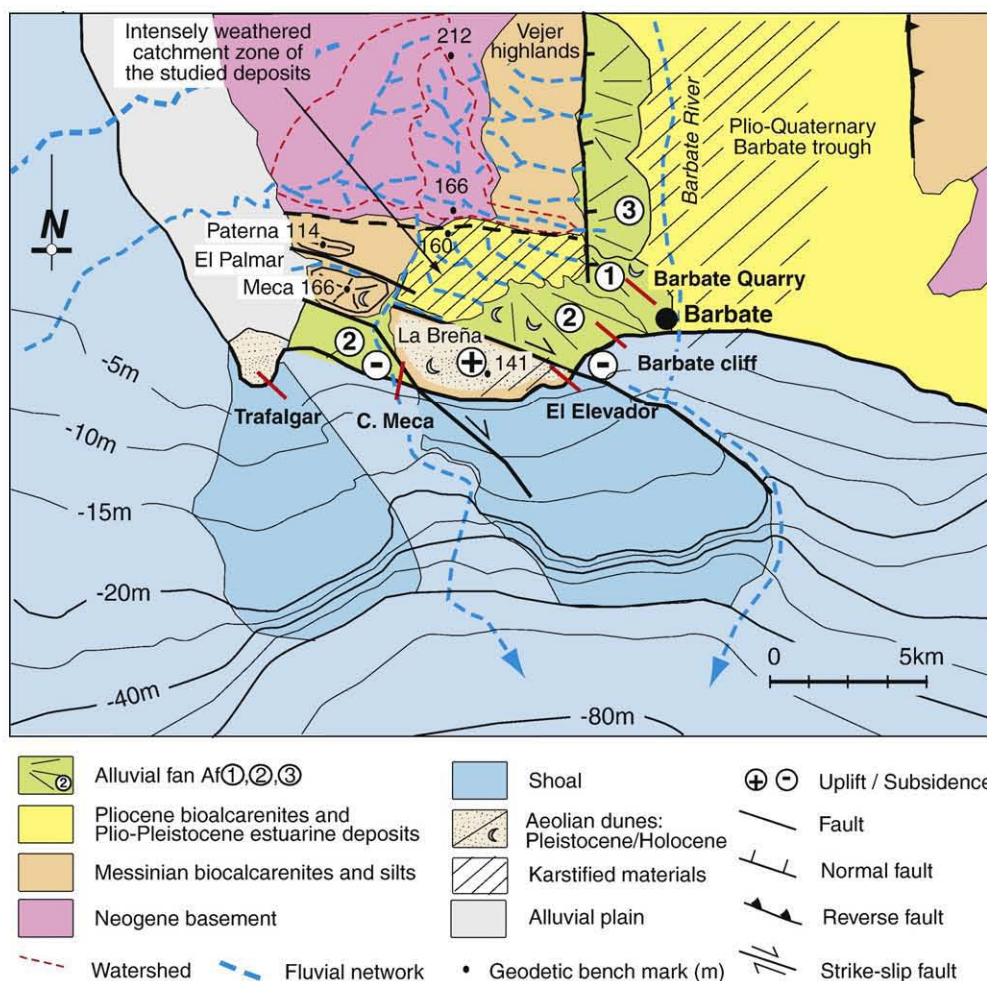


Fig. 2. Geomorphological map of the coastal sector between Barbate and Cape Trafalgar. Red, thick segments: studied sections. Topography and morphology of the continental shelf after Menanteau et al. (1989).

SE; the former are of major importance in wave generation, whereas the latter play a major role in sediment transport. The average tidal range is about 2 m.

### 3. Methodology

#### 3.1. Mapping

Geomorphological mapping (based on previous geological mapping: Zazo and Goy, 1990) offers an undated but detailed picture of the three alluvial fan systems (1 to 3 in ascending stratigraphical order), drainage pattern, and source areas (Fig. 2). The fan morphology is still visible in the younger generation of fans (Af3) which in places overlap the fans of the first generation (Af1). However, the present study is focused on the analysis of the second generation of fans (Af2). Two aeolian dune systems (Pleistocene and Holocene) cover a large part of the older fan surfaces (Af1 and Af2), and have been labelled with two different symbols in the presented map (Fig. 2). The marine deposits are always covered either by alluvial or aeolian sediments, although they crop out in the vertical walls of the cliff where the stratigraphic sections were measured and information about the neotectonic activity was obtained (Barbate cliff, El Elevador, Caños de Meca and Trafalgar). The topographic elevations reached by the transgressive maximum were measured in metres using the high-tide mark as zero datum, and appear in sections as figures preceded by a + symbol. Values in the text and figures are expressed in metres above sea level (asl).

#### 3.2. Magnetic susceptibility, mineralogy, and geochemistry

These analyses were carried out on samples collected in the Barbate Cliff and Barbate Quarry sections (Fig. 2).

Field values of magnetic susceptibility (MS) were determined with a Bartington MS2F susceptibility meter. The mineral phases were determined by X-ray diffraction (XRD) with a Philips PW-1710 diffractometer in the  $2\theta$  range from  $2^\circ$  to  $65^\circ$ . In addition, the  $<63 \mu\text{m}$  fraction of all samples was analyzed in oriented aggregates submitted to ethylene-glycol saturation and preheated up to  $110^\circ\text{C}$ . Specific XRD profiles from  $2^\circ$  to  $18^\circ$  ( $2\theta$ ) were used to discriminate the principal clay mineral species.

Geochemical analyses were carried out by means of Phillips energy-dispersive XRF analysers at the Museo Nacional de Ciencias Naturales (MNCN, Madrid) and the Geography Department of Liverpool University (UK). Bulk sample geochemistry was determined in a Metorex (Finland) isotope-source, energy-dispersive XRF analyser. The equipment uses gas-filled proportional counters with  $^{109}\text{Cd}$  and  $^{57}\text{Fe}$  gamma sources, and the resulting spectra are deconvoluted, corrected for mass attenuation effects and calibrated with standard river sediments and soils using the DECONV (Boyle, 1999) computer program.

#### 3.3. Soil analysis

Undisturbed samples for micromorphological soil study were collected from Barbate Cliff and Barbate Quarry sections (Fig. 2). Thin sections were studied using a polarizing microscope as described by



Bullock et al. (1985) and Stoops (2003). Colours of paleosols were referred to the Munsell Colour Chart. Soils were analyzed according to USDA Soil Laboratory Methods (2004). These analyses are still underway.

### 3.4. Luminescence analysis

Fourteen samples were selected for OSL. Samples of the marine deposits were collected in Barbate Cliff and Caños de Meca sections. Samples of alluvial fans came from Barbate Cliff and Barbate Quarry. The aeolian deposits were sampled in the cemented sandstones of Cape Trafalgar, and the cemented-in surfaces of Barbate Cliff, El Elevador, and Barbate Quarry.

Most samples were taken by inserting duralumin pipes in clean, freshly-cut sections to avoid exposure of the grains to light. However, an exception was made for sample TF03-1 because the sediment was brecciated; in this case, a brick-sized block ( $\sim 20 \times 10 \times 10$  cm) was chiselled from the face.

Environmental gamma and cosmic dose-rates were measured *in situ* with a portable spectrometer equipped with a NaI detector.

## 4. The sedimentary record

The basement of most of the studied sections is a Messinian biocalcarenite with silty deposits, except in Barbate Quarry where it is not exposed. Three sedimentary units – marine, alluvial, and aeolian – are usually present in all sections.

### 4.1. The studied sections

In the cliffs separating the villages of Barbate and Caños de Meca (Fig. 2), the most complete sections are found in the areas of El Elevador, the harbour of Barbate, and in Caños de Meca. These two sites are separated by the “La Breña”, an uplifted platform which is made up of deeply weathered Messinian calcarenites. Not far to the west is the tombolo of Trafalgar Cape where the facies are somewhat different, since only the marine and aeolian deposits are present. The difference is related to the different geomorphologic setting. The section at Barbate Quarry is located north of the village of Barbate, and is composed of reddish alluvial sand deposits. Zazo (1980) and Zazo and Goy (1990) interpreted these deposits as glacial, but assigned them an age older than those exposed in the cliffs, despite the similarity of the facies.

Most laboratory work was carried out on samples collected in Barbate Cliff (Fig. 3) and Barbate Quarry (Fig. 5). The other sections provided chronologic and paleoenvironmental information.

#### 4.1.1. Barbate Cliff

The Messinian substratum (Fig. 3A, B) is topped by a rock platform which, in turn, is covered by basal conglomerate that passes upwards into shoreface–foreshore calcarenitic facies. The transgressive maximum of these beach facies reaches 3.5 m asl. Intense cementation and karstification recrystallized much of the faunal evidence. Consequently, it is difficult to identify the fauna at species level. U–Th analysis gave an age  $84 \pm 4 / -9$  ka (Zazo, 1980; Zazo et al., 1999).

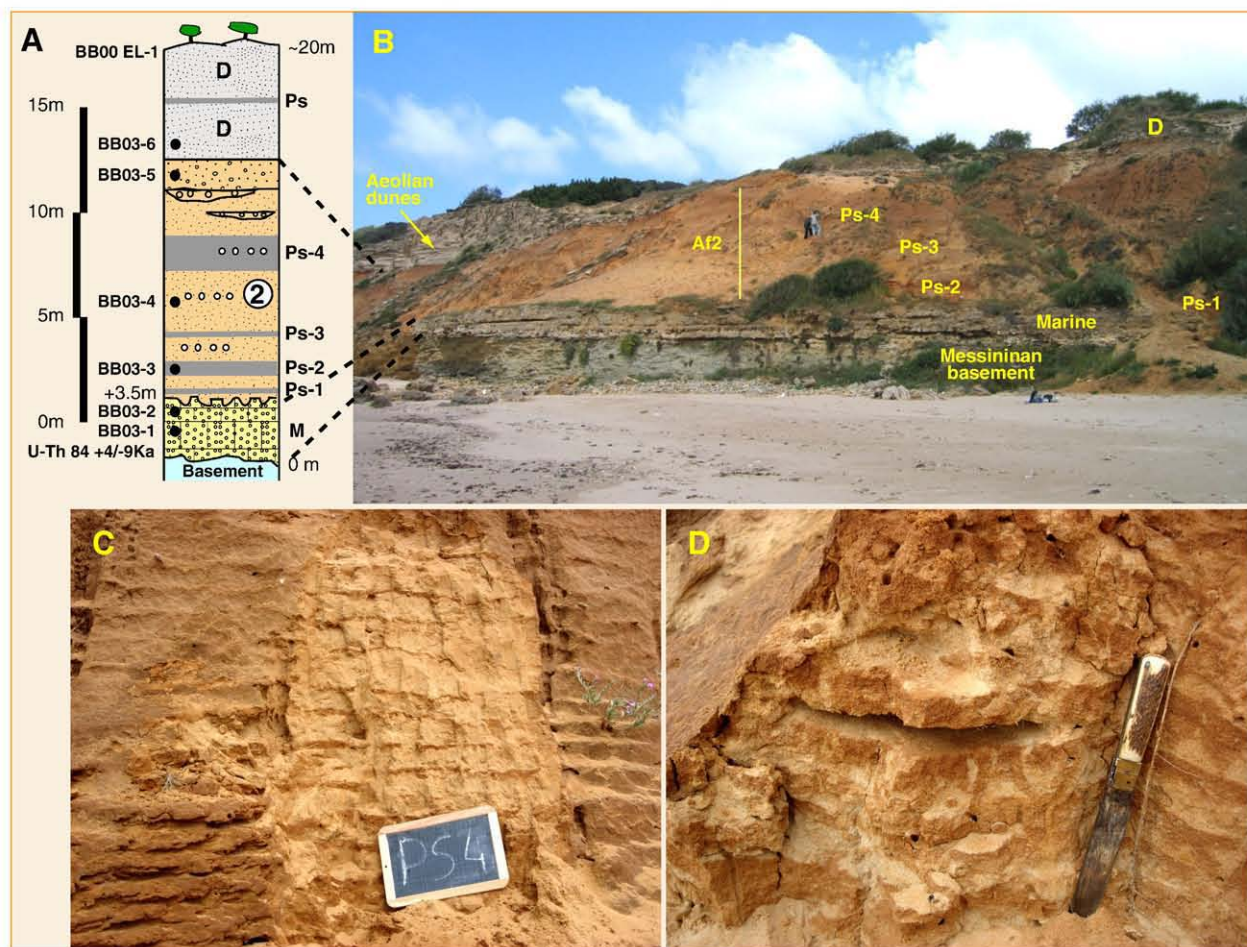


**Fig. 3.** (A) Stratigraphic section, and (B) panorama of Barbate Cliff section: (M), marine deposits; (Af2) Alluvial fan of the second generation; (D): Aeolian dunes; Ps: Paleosols; BB00, BB03...: location of OSL samples; (+3.5 m): topographic elevation asl of the transgressive maximum of marine deposits; (C and D): lamellae in the lower (C) and upper (D) part of Ps-4 soil profile (length of knife: 25 cm; portable slate:  $25 \times 18$  cm).



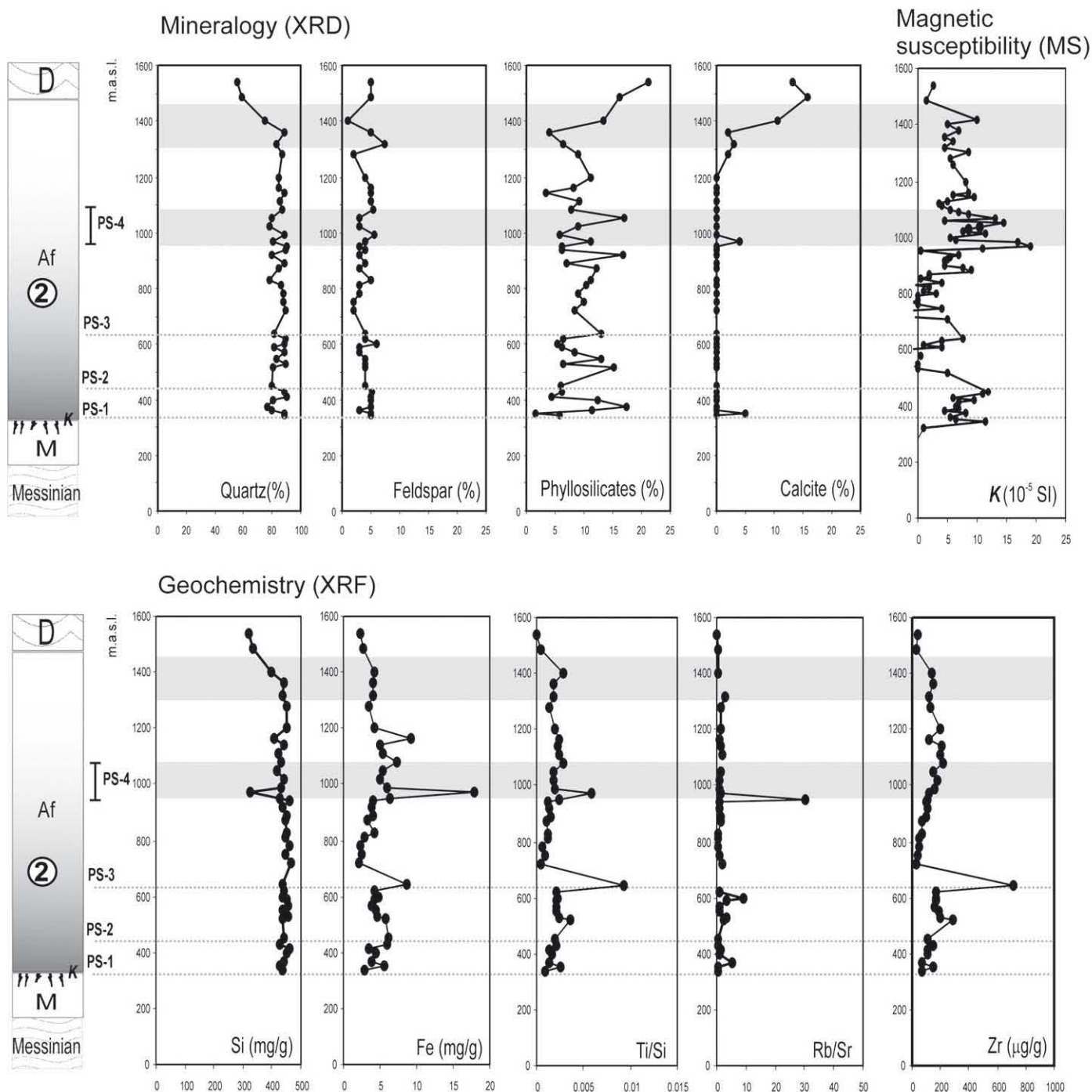


Fig. 4. Logs of the Barbate Cliff section, with results of mineralogical, geochemical and magnetic susceptibility analyses.

The marine unit is unconformably covered by reddish sandy deposits with thin gravel interbeds (lags and channel-shaped bodies) that become more abundant towards the top. This unit has been interpreted as alluvial fan deposits (Af2) with sheet-flood facies. The most outstanding feature throughout the alluvial sequence is the pervasive occurrence, particularly towards the top, of repetitive red bands (lamellae) that had not been described before in this region. The top of the alluvial unit is a sharp, erosional boundary.

The youngest deposits in this section are aeolian dune sands, typically cemented at the surface. There are two overlapping dune units separated by a burrowed root layer (Ps). The estimation of the prevailing paleowind direction in the lower unit is from the SE, and in

the upper unit from the south. The dune forms immediately below the mobile Holocene ones are barchans.

Most prominent within the alluvial reddish sands are the four main paleosols (Ps-1 to Ps-4). These are a result of the coalescence and aggregation of red clay bands (clay lamellae), particularly in the case of Ps-4 which displays alternating yellowish (5YR 5/8m) and red (2.5YR 4/6m) bands (Fig. 3C). In this case the lamellae thickness and spacing vary from the base to the top of the soil profile. Thin lamellae (ca. 1 cm) separated by relatively thick intervals (ca. 8 cm) prevail in the base of the profile (Fig. 3C), whereas thicker lamellae (6 cm or more) separated by thinner intervals (3–4 cm) are characteristic of the upper part (Fig. 3D). The clay content in the red bands (5–6%) is higher



than in the yellowish ones (1–2%). Micromorphological analyses reveal the occurrence of clay-bridged or clay-pellicular grain microstructures as consistent indicators for the pedogenic origin of the red banding. The main soil-forming process is clay illuviation, as recorded in pedofeatures such as well-oriented clay coatings (grain and pores) and scarce clay microlaminations.

XRF, XRD and magnetic susceptibility analyses of the Barbate Cliff section allow these paleosols to be characterized (Fig. 4). Mineralogy is mainly quartz, with scarce feldspar, but weathered clays may amount up to 20% of the weight in some samples. Phyllosilicates are always clay minerals with a predominance of illite (up to 15%), lower values of montmorillonite and kaolinite (less than 5%), and traces of clinocllore. Paleosols are identified in the geochemical results by increased values of Ti, Fe and Zr which are indicative of pedogenic enrichment, mainly illuviation. The Ti/Si ratio characterizes the variation in clay minerals, and serves as an indicator of eluviation (Fig. 4). The Rb/Sr ratio is a useful indicator of the intensity of pedogenesis (Chen et al., 1999; Sangode and Bloemendal, 2004). Noticeable increases of magnetic susceptibility (MS) in the red horizons (Ps-1 to Ps-4) indicate the increase of ferromagnetic particles associated with pedogenesis. The final phases of alluvial fan sedimentation are reflected in mineralogy by a decrease in quartz and feldspar content, increased calcite and, at the top, a marked increase in phyllosilicates. These changes, along with a relative increase in the Ti/Si ratio, are additional indicators of a major eluviation/leaching period.

The occurrence of four paleosols in the alluvial deposits indicates a reduced supply of sediment to the alluvial fans, and suggests repeated periods of increased aridity that favoured rubefaction.

Overlying the alluvial sediments are aeolian dune deposits which are mainly composed of quartz particles partially cemented by carbonates. Magnetic susceptibility is low due to the absence of ferromagnetic particles (Fig. 4).

#### 4.1.2. Cantera de Barbate

The sedimentary sequence exposed in the Barbate Quarry (Fig. 5) begins with reddish sands scattered with quartz and quartzite

pebbles, and belonging to the first generation of fans (Af1: Figs. 2 and 5, see Zazo and Goy, 1990). The top of this unit still preserves the remains of a 60 cm-thick red paleosol (Ps-1). The following unit (in ascending stratigraphical order) consists of pale brown sands with interbedded discontinuous gravel layers (A, in Fig. 5), interpreted as alluvial deposits. The boundary with the underlying unit is erosional.

The uppermost unit consists of well sorted, whitish sands with large sets of high-angle cross-bedding, interpreted as aeolian dunes. They are essentially uncemented, although a superficial cementation gives them a weather-resistant appearance. Two dune systems are distinguished, separated by an organic-rich grey layer (Ps in Fig. 5). Paleowind directions deduced from cross-bedding are from SE and E (lower unit), and E (upper unit). Man-made lithic artefacts recovered immediately above the boundary between alluvial and aeolian dune sediments have been identified as Neolithic–Chalcolithic, which in this region is dated between 6 and 4 ka BP (Martín de la Cruz et al., 2000).

Partial erosion of the paleosol (Ps) does not permit any detailed study. Where a significant part of the soil profile is preserved, it consists of a structureless, reddish-yellow (5YR 5/8d) sandy horizon, with little red mottles (2.5YR 4/8d). Texture and colour change downwards to a sandy and loose horizon which is 7.5YR 5/8d in colour. A stratigraphically-lower red (2.5YR 4/8d) soil horizon, with no visible structure, is exposed in some parts of the quarry. This horizon is a sandy clay loam with clay content up to 15%, thought to represent the maximum degree of evolution.

The mainly siliciclastic alluvial fan (Af1) and alluvial (A) deposits (Fig. 6) have undergone incipient illuviation, as indicated by the occurrence of Mn oxides (probably todorokite) and increased Ti and MS. Increased phyllosilicate content suggests that pedogenic processes were more intense in Af1.

Low values of magnetic susceptibility result from mineralogy, dominated by quartz. Three peaks record local increases in ferromagnetic minerals. An even more marked peak (a few centimetres below the other three) is thought to indicate a noticeable increase in ferrimagnetic particles, such as iron oxides. The highest values of MS were found just below the red paleosol (~570 cm in the section)

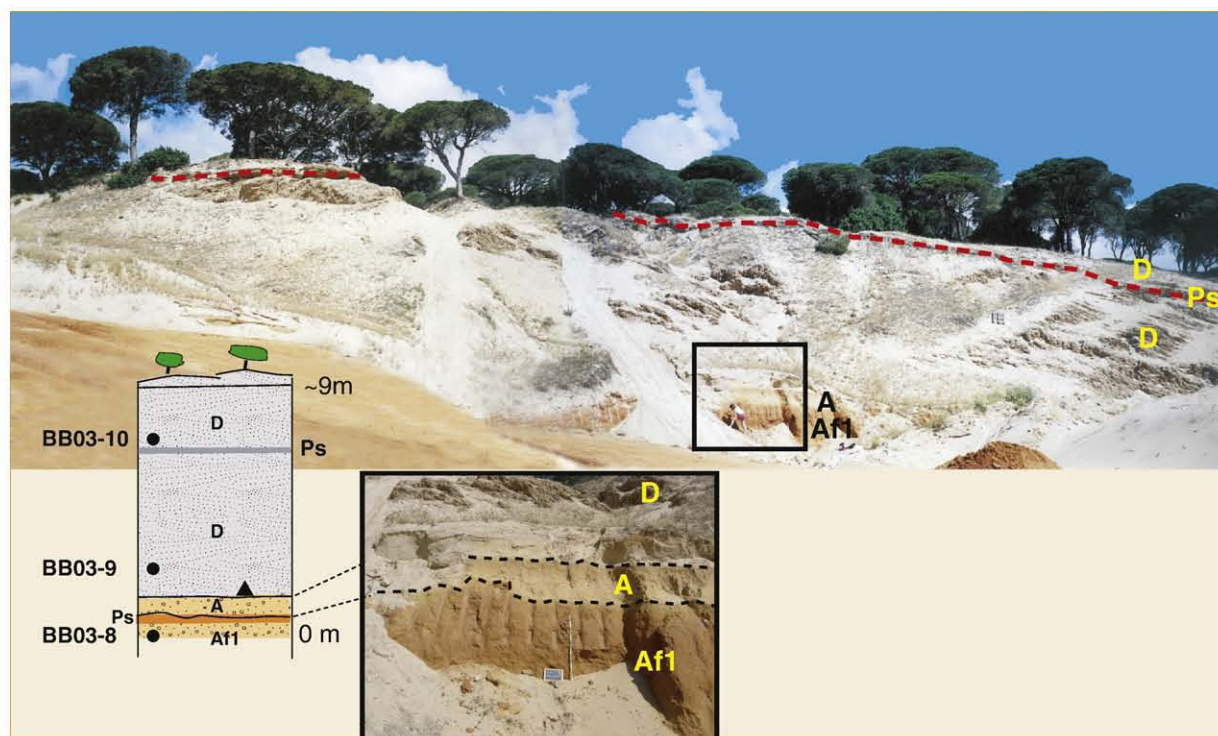


Fig. 5. Panorama, stratigraphic section, and close up of Barbate Quarry: deposits of alluvial fan (Af1); (A): Alluvial; (D): Aeolian dunes; (Ps): Paleosol; black dots marked BB03–8, 9, and 10 denote the location of OSL samples. Black triangle: man-made artefacts.



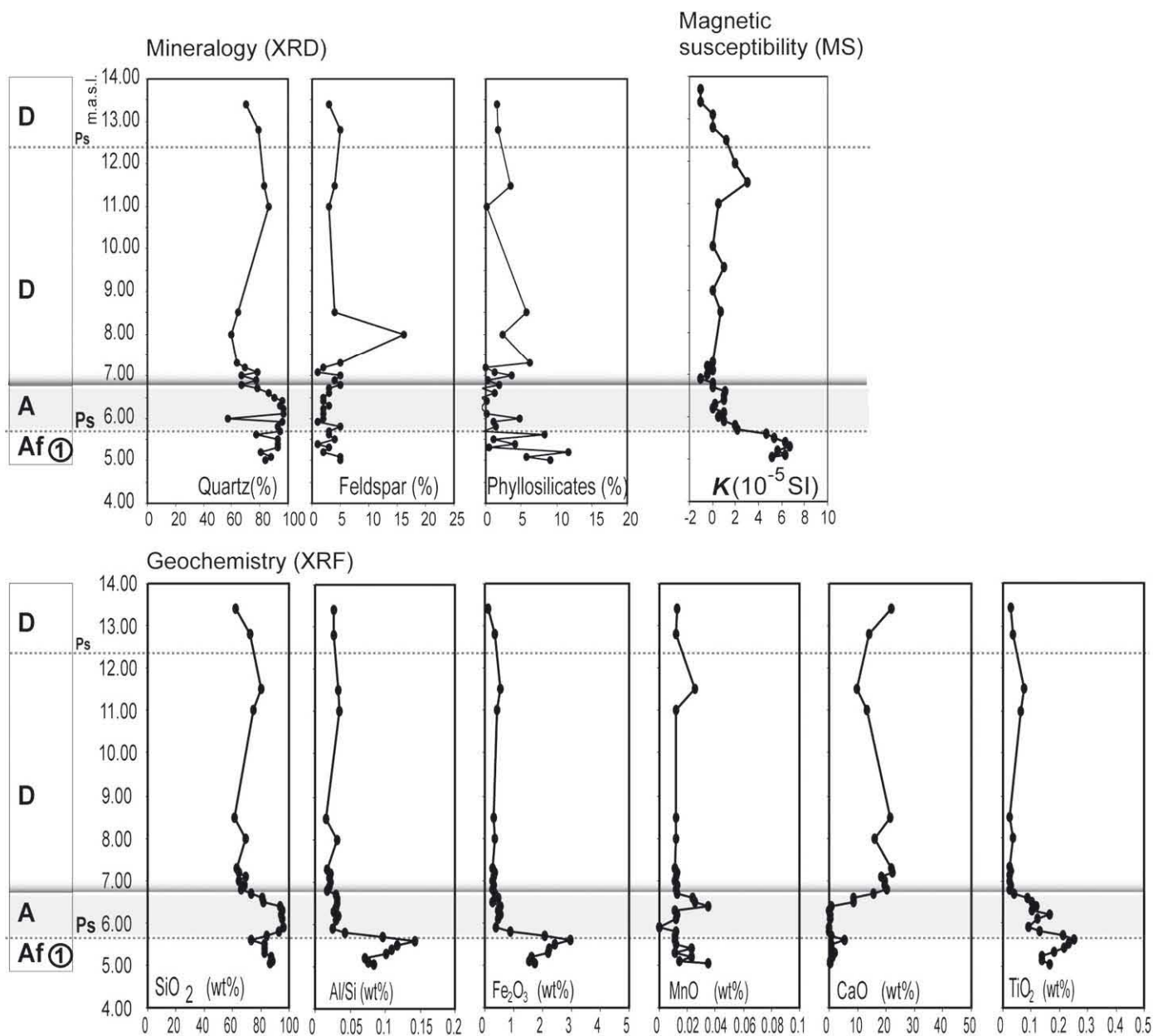


Fig. 6. Logs of the Barbate Quarry section, with results of mineralogical, geochemical and magnetic susceptibility analyses.

coinciding with high values of Al, Fe and Ti. The observed increase in the Al/Si ratio, an indicator of eluviation in soils (Sangode and Bloemendal, 2004), suggests a long lasting pedogenetic process.

The aeolian sediments are also siliciclastic. The lowermost part of the older dune (between 680 and 730 cm) is more cemented, as indicated by increased Ca and Mg. The thin layer separating the two dune systems (Ps at ~920 cm, Figs. 5 and 6) also underwent eluviation processes and exhibit increased Al, Fe, Mn, Ti, ratio Al/Si, and MS. The preservation of some metallic cations (Na, K, Ca, Mg) suggests that eluviation was discontinuous and/or incomplete. The increase in phyllosilicate (mainly kaolinite) content, together with geochemical and magnetic data, suggests pedogenic processes. Therefore, this layer is considered to represent a paleosol (Ps in Fig. 5).

#### 4.2. OSL dating

All the environmental gamma dose-rates range from ~150 to 300  $\mu\text{Gy/a}$  (Table 1) and are typical of sandy sediments rich in

minerals like quartz and, to a lesser extent, carbonates and clays. In the laboratory, a fraction of each sample was also analyzed with a high purity Ge detector to determine its radioisotopic contents (U, Th and K – Table 1) and to ensure that the radioactive U- and Th-series were in secular equilibrium.

Due to the abundance of quartz grains, this mineral fraction was selected by wet sieving in order to remove most of the clay. HCl and HF treatments allowed us to eliminate carbonates and to clean the surface of the quartz grains (Zazo et al., 2005). Sub-millimetre grains were then used to estimate the radiation dose which they had accumulated since they were last exposed to light. For each sample, this equivalent dose (ED) was measured on several aliquots (between 12 and 48 – Table 2) with a Single-Aliquot Regenerative-dose (SAR) protocol (Murray and Wintle, 2000), and the individual values were plotted on a histogram. Fig. 7 gives examples of such histograms for samples BB03–9, CM03–2 and BB03–3, chosen for their significant variance in EDs (from ~5.40 to 90 Gy). As expected, the shape of each histogram depends on the number of aliquots and on the scatter of the

**Table 1**  
Radioisotopic contents of the sediment samples measured in the laboratory by gamma spectrometry using a Ge detector

Sample ref.	Radioisotopic contents						Environmental dose-rates ( $\mu\text{Gy/a}$ )	
	U (ppm)	$\pm$	Th (ppm)	$\pm$	K (%)	$\pm$	Gamma	Cosmic
<i>Barbate Cliff</i>								
BB00EL1 (D)	0.63	0.03	0.88	0.05	0.28	0.01	141	170
BB03-6 (D)	0.41	0.02	0.65	0.03	0.22	0.01	165	160
BB03-5 (Af.2)	0.41	0.02	1.35	0.05	0.52	0.01	181	160
BB03-4 (Af.2)	0.41	0.02	1.28	0.03	0.31	0.01	165	50
BB03-3 (Af.2)	0.43	0.02	1.50	0.08	0.71	0.02	273	50
BB03-2 (M)	0.49	0.03	0.56	0.04	0.34	0.01	215	50
BB03-1 (M)	0.60	0.03	1.33	0.05	0.69	0.01	215	50
<i>Barbate Quarry</i>								
BB03-10 (D)	0.44	0.02	0.96	0.05	0.80	0.01	208	160
BB03-9 (D)	0.41	0.02	0.93	0.03	0.70	0.01	208	160
BB03-8 (Af.1)	0.72	0.02	3.10	0.03	0.79	0.02	319	160
<i>El Elevador</i>								
BB03-7B (D)	0.47	0.02	1.15	0.05	0.30	0.01	221	160
BB03-7A (D)	0.42	0.02	1.01	0.03	0.27	0.01	176	160
<i>Caños de Meca</i>								
CM03-2 (M)	0.43	0.01	0.77	0.04	0.43	0.01	188	110
CM03-1 (M)	0.54	0.01	1.17	0.04	0.81	0.01	204	92
<i>Trafalgar</i>								
TF00EL1 (D)	0.60	0.02	0.45	0.03	0.18	0.01	149	123
TF03-1 (D)	0.35	0.03	0.75	0.04	0.56	0.02	186	63

These values allowed calculating the contribution of the alpha and beta radioactivity to the annual dose-rate, which also includes the gamma and cosmic components measured in the field with a portable NaI detector. When in situ measurements were not possible (as for sample TF03-1) the gamma component was calculated from the radioisotopic contents and the cosmic dose-rate was estimated after Prescott and Hutton (1988).

individual ED values, which may reflect microdosimetric effects and indicate the presence of poorly bleached grains (i.e. grains insufficiently exposed to sunlight before burial). In all cases, the mean ED (Table 2) was calculated by averaging all the individual values except when some of them were statistically different from the mean. This was the case for sample BB03-3 where the outlying values were discarded before the calculation of the mean ED.

Table 2 gives the OSL age estimates calculated by dividing the mean ED by the annual dose-rate: they range from  $137 \pm 17$  ka for BB03-8 to less 1 ka for BB00EL1. The OSL ages are coherent with the stratigraphy and with the U-Th dates already available (Zazo, 1980; Zazo et al., 1999).

The results of OSL and U-Th dating, coupled with sedimentological data and the updated map, allowed us to refine the chronological evolution of the Barbate-Trafalgar region.

According to OSL and U-Th data, the marine sediments below the alluvial fan sequence are of last interglacial age or OIS 5, but the data are inadequate to discriminate between OIS 5e or OIS 5c. Arguments in favour of OIS 5e are the widely accepted higher mean sea level, estimated in  $\sim 5$  m asl along stable coasts during OIS 5e (Muhs et al., 2002), and the existence of more than one highstand at the same time (e.g. Bard et al., 1990). This is also recognized in the Spanish Mediterranean coasts between  $\sim 135$  and  $117$  ka (Hillaire-Marcel et al., 1996; Zazo et al., 2003) but always with similar highstand elevations. In contrast, on the Atlantic coasts of Spain the deposits of OIS 5e and 5c are known (so far) to be single highstands bearing Senegalese warm faunas, with U-Th ages  $\sim 128$  ka and  $\sim 95$  ka respectively (Zazo et al., 1999).

The present maximum elevations reached by the last interglacial deposits in the Gulf of Cadiz range between  $19.5$  m (Tarifa) and  $12$  m (west of Barbate and El Palmar, Fig. 2) for the OIS 5e, and between  $11$  m

(Tarifa) and  $8$  m for the OIS 5c (Zazo et al., 1999, 2003). In the absence of consensus about the paleo-position of sea level during OIS 5c, and more precise dating in the study area, it seems reasonable to assign the marine deposits between Barbate and Trafalgar to the OIS 5c.

Concerning the alluvial fan deposits, the oldest sequence is located at Barbate Quarry (Af1 in Fig. 2) where the topmost layer was dated at  $137 \pm 17$  ka. The alluvial fan in Barbate-Meca belongs to the second sequence (Af2), dated  $\sim 112 \pm 14$  to  $\sim 12.0 \pm 1.2$  ka. The most recent alluvial fan system (Af3 in Fig. 2) which still preserves the surface morphology, and has not been significantly affected by pedogenesis, is assigned a Holocene age.

The age of the aeolian deposits is Holocene, except for those outcropping in the Trafalgar Cape. They are older, as deduced from their higher degree of induration and OSL ages (Fig. 8). The absence of alluvial deposits here is mainly due to their particular location, in the sense of their orientation and isolation with respect to the catchment area. Fig. 8 summarizes the correlation between the different sedimentary sequences.

#### 4.3. Paleogeographical evolution and climate

The oldest alluvial fan (Af1) in Barbate Quarry (Figs. 2, 5) was deposited during the latest part of the OIS 6, and underwent pedogenesis under a temperate, moist climate with red soil forming probably during the peak of OIS 5e. There then followed an arid period, similar to that recorded along the Atlantic coast of Iberia during OIS 5d (Sánchez-Goni et al., 1999). During the ensuing highstand (OIS 5c), upper shoreface and beach units were deposited along a coastline very much like at present, as deduced from detail mapping of the transgressive maxima.

**Table 2**  
Annual dose-rates, equivalent doses, and OSL age estimates for the Barbate samples

Sample ref.	Annual dose-rate		Equivalent dose		n	SAR protocol	OSL age	
	( $\mu\text{Gy/a}$ )	$\pm$	(Gy)	$\pm$			(ka)	$\pm$
<i>Barbate Cliff</i>								
BB00EL1 (D)	613	25	0.5	0.1	24	220°,10° 160°,0°	0.77	0.10
BB03-6 (D)	526	19	3.0	0.2	24	250°,10° 160°,0°	5.7	0.6
BB03-5 (Af2)	666	19	8.6	0.5	24	Id	12.9	1.2
BB03-4 (Af2)	487	18	50	2	48	Id	102	10
BB03-3 (Af2)	860	30	96	8	24	Id	112	14
BB03-2 (M)	558	12	63	2	24	240°,10° 160°,0°	113	10
BB03-1 (M)	804	24	87	6	24	250°,10° 160°,0°	108	12
<i>Barbate Quarry</i>								
BB03-10 (D)	848	22	5.6	0.3	24	Id	6.7	0.6
BB03-9 (D)	792	22	5.3	0.2	24	Id	6.7	0.6
BB03-8 (Af1)	1016	34	139	13	48	250°,10° 160°,0°	137	17
<i>El Elevador</i>								
BB03-7B (D)	651	25	3.4	0.2	24	220°,10° 160°,0°	5.2	0.5
BB03-7A (D)	578	19	5.0	0.2	24	Id	8.7	0.7
<i>Caños de Meca</i>								
CM03-2 (M)	644	12	40	1	12	240°,10° 160°,0°	62	5
CM03-1 (M)	918	12	93	3	12	Id	101	9
<i>Trafalgar</i>								
TF00EL1 (D)	488	25	38	2	24	220°,10° 160°,0°	78	8
TF03-1 (D)	676	8	67	5	24	240°,10° 160°,0°	99	12

(n): number of aliquots measured using the SAR protocol which allows comparing the natural OSL signal to signals regenerated with artificial doses. The preheat treatments (between  $220$  and  $250$  °C for  $10$  s) used prior to OSL measurements are indicated. Treatments used for measurement of a test dose ( $160$  °C for  $10$  s) necessary for correcting sensitivity changes which might happen during the aliquot analysis are indicated as well. Note that for the Annual Dose-rate and Equivalent Dose, the uncertainties are based on statistical errors only and do not include systematic errors, whereas for the OSL ages the uncertainties combine both statistical and systematic errors.



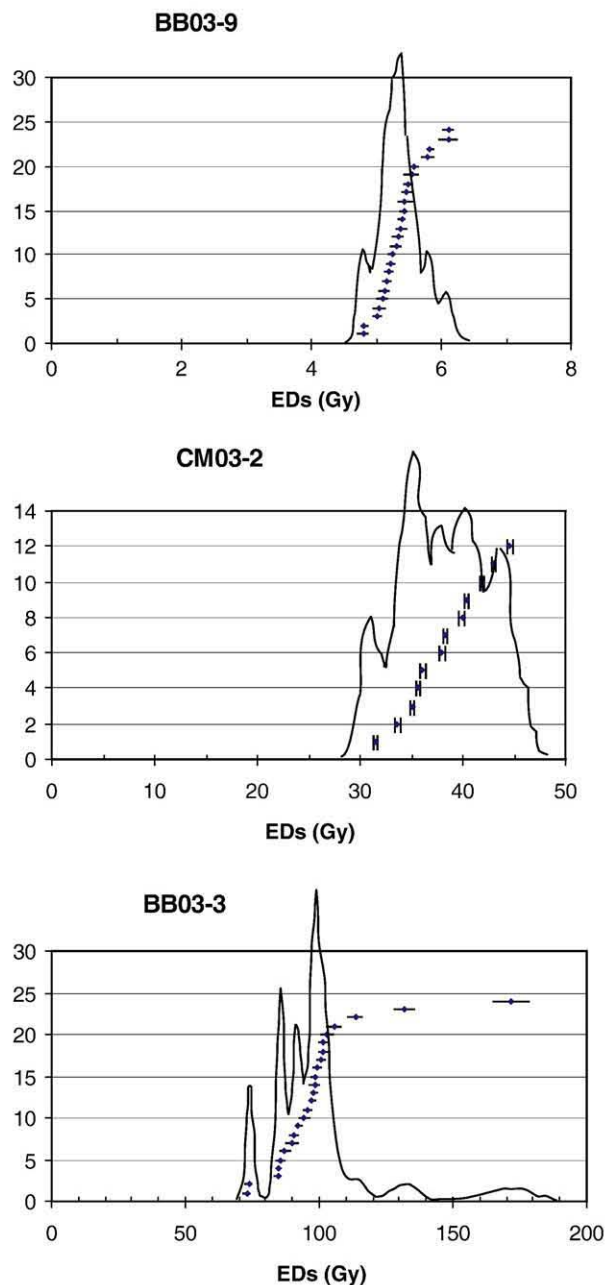


Fig. 7. Histograms of the individual ED values represented by the dots for samples BB03-9, CM03-2, and BB03-3. The number of aliquots was 24, 12 and 24, respectively.

Continued activity of the NE-SW-oriented faults led to subsidence in Barbate and Meca, separated by the uplifting La Breña area. Subsidence favoured the accumulation of the second generation of alluvial fans (Af2, Figs. 2, 3) under conditions moister than before. The source area of these fans includes the karstified Mio-Pliocene calcarenites and the reddish Plio-Pleistocene estuarine sandy deposits, forming small catchment areas (Fig. 2). In the best exposed outcrops of the Barbate fans up to five sedimentary phases are distinguished, which are separated by paleosols (Ps-1 to Ps-4). Paleosol Ps-4 consists of lamellae and marks the end of the fourth alluvial fan phase. It was generated after a relatively moist period. The growth of the fan was favoured by an alternating moist/arid climate that culminated in a long lasting arid period that favoured the reddening of the stratigraphically higher thick red bands (Fig. 3D).

Putting together the described succession of events and the available OSL ages, we conclude that the first four phases of fan growth took place during the late OIS 5 interglacial, and that the prolonged, more arid period corresponds to the passage from OIS 4 to OIS 3. Pollen studies in the coastal areas of the Gulf of Cadiz indicate that by OIS 3 times the region had passed from a markedly arid period to more humid conditions (Yll et al., 2003). The last (fifth) phase of fan development must be placed in OIS 3 and the tardiglacial (OIS 2), with more humid conditions recorded by the increased number of channel bodies towards the top. The occurrence of lamellae indicates a new recurrence of arid periods.

Recent works summarized in Macklin et al. (2002) show that alluviation was intense in fluvial and alluvial environments of the western Mediterranean during OIS 5b and 5a. In this case alluvial accumulation started at times with a relative high sea level, but not during the peak of the interglacial highstands when coastal erosion worked at fan toe locations promoting the generation of cliffed coasts (Harvey et al., 1999), as is the case of the modern Barbate-Trafalgar cliff generated during the present interglacial. Therefore, the conjugation of the broad sea-level retreat from OIS 5c to OIS 2, with the occurrence of subsiding zones along NW-SE fault partially damming the alluvial-coastal connection favoured the accumulation of the thick sedimentary sequence of repeated sheet-flood deposits. It should be noted that the only visible sedimentary record outcrops in the cliff (at relatively ancient proximal locations), so inferences of processes occurring at distal fan locations during lower positions of sea level are less clear.

There is no evidence of major dissection during the glacial periods, only repeated processes of sedimentation and pedogenesis at least over the more proximal zones of the ancient coastal fan area during both glacial and interglacial periods. The climatic alternation recorded both during glacial and interglacial periods is preserved in the sedimentary record as oscillations in the humidity/aridity ratio, with no remarkable changes in temperature. The study of marine cores in the Atlantic-Mediterranean linkage area has revealed a high climatic variability during the last 250 ka that is recorded both in atmospheric and oceanic conditions (Sánchez-Gómez et al., 1999; Cacho et al., 1999, 2002; Sánchez-Gómez et al., 2002; Martrat et al., 2004).

The end of activity of the coastal alluvial fans (Af2) is probably related to a regional increase of aridity that eventually led to hydrological inactivity and the progressive invasion of fans by aeolian dunes around 8 ka BP. Additional proof of this event is a short-lived drop of water-lake levels in Lake Medina, not far away to the NW (Reed et al., 2001). Since that time, the regional trend to increased aridity led to widespread regional aeolian accumulation after 5 ka (Goy et al., 2003; Zazo et al., 2005). The poorly developed greyish paleosols that separate the aeolian dune systems indicate somewhat more humid periods that punctuate the general arid trend.

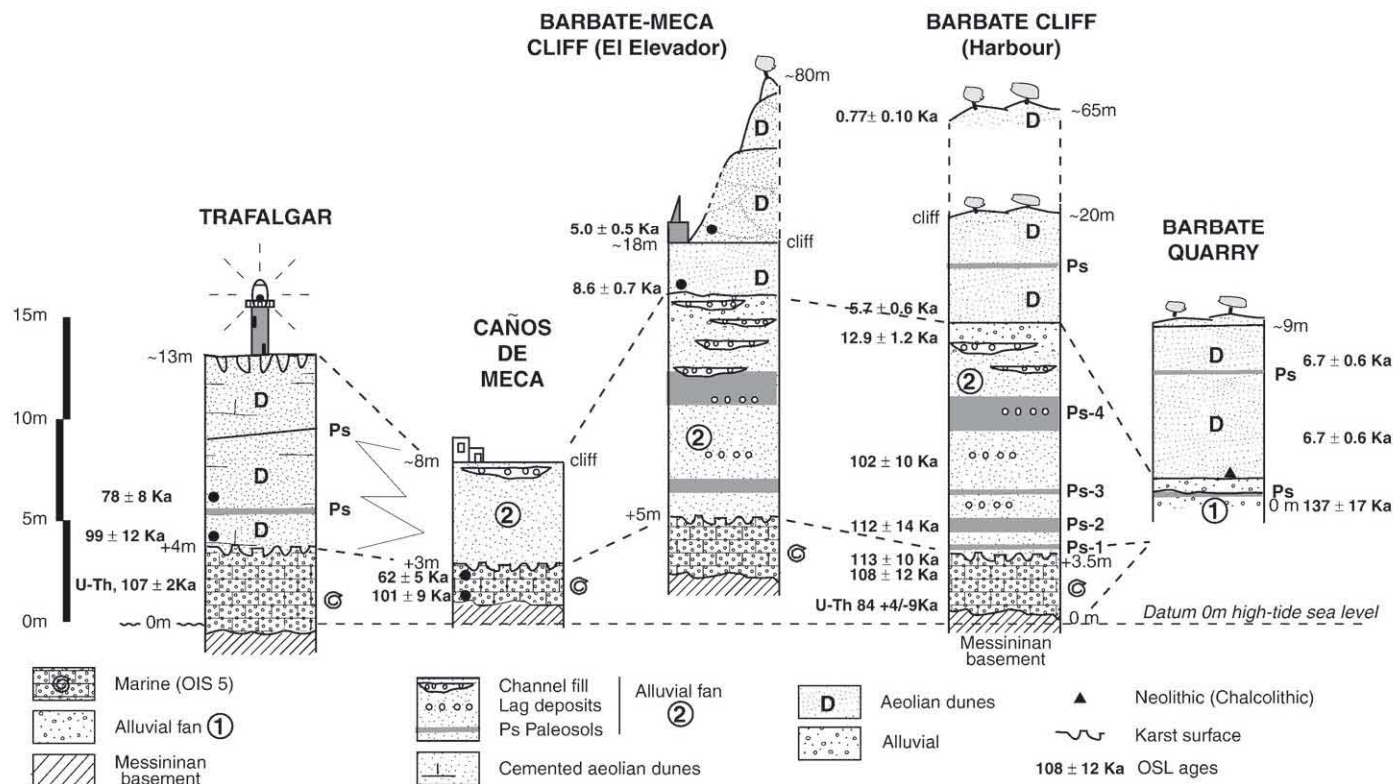
## 5. Conclusions

The main factors controlling the occurrence of marine, alluvial fan, and aeolian late Pleistocene to Holocene units distinguished in the northern coast of Gibraltar Strait are tectonics, eustasy and climate.

The tectonic factor controlled the location of alluvial fans in places adjacent to the NW-SE faults that generated uplifted highlands and subsiding troughs, and pre-determined the drainage network through which sediment was transferred from the catchment areas to the fans. The tectonic activity also controls the present topographic elevations of the OIS 5c marine sediments and the morphology of the inner continental shelf.

The climatic factor controlled the sediment supply to the coast and the pedogenic processes that generated the red paleosols interbedded in the alluvial fan deposits. Up to five aggradational phases have been recognized in the most complete fan (Af2) with intervening periods of inactivity that coincided with episodes of marked aridity and paleosol generation. The best developed paleosols are Ps-2, which formed





around the end of the last interglacial, and Ps-4, with final phases of development coinciding with a remarkable arid period that we tentatively place around the end of OIS 4. The last (fifth) episode of fan growth took place during a more humid period that favoured the enlargement of the channel network, as evidenced by the increasing upward abundance of gravel lag and channel-fill facies. We correlate the last phase with OIS 3 and the tardiglacial. The almost continuous occurrence of lamellae intercalations in the sandy parent material suggest that the humid climatic conditions that favoured the supply of sediment to the fans were followed by alternating humid and arid periods; the first promoted clay illuviation, and the second the reddening of lamellae.

According to the few OSL ages available, most sediment was delivered to the coastal zone during the end of the penultimate and last glacial periods, and the last part of the last interglacial period; that is to say, at times when sea level was high but not at highstand or lowstand peaks.

The second generation of alluvial fan (Af2) ceased to grow around 8 ka, due to increased regional aridity. The abandoned fans were colonized by aeolian dunes. Regional aridity and aeolian activity has been the norm in the Atlantic-Mediterranean zone since 5 ka, punctuated by shorter-lived less arid (somewhat more humid) periods when the sandy greyish paleosols separating successive systems of aeolian dunes accumulated.

## Acknowledgements

We are grateful to Adrian's influence. His open, well-oriented scientific spirit led him to share and discuss ideas with many of us. This research has been funded by Projects BTE 2002-1065 and BTE 2002-1691; CGL 2005-01336/BTE and CGL 2005-04655/BTE; Consolider - Ingenio 2010 - GRACCIE. It is also a contribution to Projects INQUA "Marine and Terrestrial Processes", IGCP 495, and UCM Workgroup 910198. Thanks to Drs. T. Boski and C.R. Firth who kindly reviewed and improved the manuscript.

## References

- Bard, E., Hamelin, B., 1990. U/Th ages by mass spectrometry in corals from Barbados: sea level during the past 130,000 years. *Nature* 346, 456–458.
- Benkheilil, J., 1976. Etude néotectonique de la terminaison occidentale des Cordillères Bétiennes (Espagne). Thèse 3ème Cycle. Univ. Nice.
- Bond, G., Broecker, W., Johnsen, S.J., McManus, J., Labeyrie, L., Jouzel, J., Bonani, G., 1993. Correlation between climatic records from North Atlantic sediments and Greenland ice. *Nature* 363, 143–147.
- Borja, F., 1992. Cuaternario Reciente, Holoceno y Periodos Históricos del SW de Andalucía. Paleogeografía de medios litorales y fluvio-litorales de los últimos 30.000 años. PhD Thesis, Universidad de Sevilla. 520 pp.
- Boyle, J.F., 1999. Isotope-source, energy-dispersive XRF analysis of geological materials using gas-filled proportional counters: signal deconvolution using simulated peak shapes. *X-ray Spectrometry* 28, 178–182.
- Bullock, P., Fedoroff, N., Jongerius, A., Stoops, G., Tursina, T., Babel, U., 1985. Handbook for Soil Thin Section Description. Waine Research Publications, Wolverhampton, UK.
- Cacho, I., Grimalt, J.O., Pelejero, C., Canals, M., Sierro, F.J., Flores, J.A., Shackleton, N.J., 1999. Dansgaard-Oeschger and Heinrich event imprints in Alboran Sea temperatures. *Paleoceanography* 14, 698–705.
- Cacho, I., Grimalt, J.O., Canals, M., 2002. Response of the Western Mediterranean Sea to rapid climatic variability during the last 50,000 years: a molecular biomarker approach. *Journal of Marine Systems* 33–34, 253–272.
- Chen, J., An, Z.S., Head, J., 1999. Variation of Rb/Sr ratios in the loess-paleosol sequences of Central China during the last 130,000 years and their implication for monsoon paleoclimatology. *Quaternary Research* 51, 215–219.
- Dansgaard, W., Johnsen, S.J., Clausen, H.B., Dahl-Jensen, D., Gundestrup, N.S., Hammer, C.U., Hvidberg, C.S., Steffensen, J.P., Sveinbjörnsdóttir, J., Jouzel, J., Bond, G., 1993. Evidence for general instability of past climate from a 250-kyr ice-core record. *Nature* 364, 218–220.
- Goy, J.L., Zazo, C., Silva, P.G., Lario, J., Bardaji, T., Somoza, L., 1995. Evaluación geomorfológica del comportamiento neotectónico del Estrecho de Gibraltar (zona Norte) durante el Cuaternario. IV Coloquio Internacional sobre el enlace fijo del Estrecho de Gibraltar, Sevilla 1995. I Medio Físico. SECEG, S.A. Madrid, pp. 55–69.
- Goy, J.L., Zazo, C., Dabrio, C.J., 2003. A beach-ridge progradation complex reflecting periodical sea-level and climate variability during the Holocene (Gulf of Almería, Western Mediterranean). *Geomorphology* 50, 251–268.
- Harvey, A.M., Silva, P.G., Mather, A.E., Goy, J.L., Stokes, M., Zazo, C., 1999. The impact of Quaternary sea-level and climatic change on coastal alluvial fans in the Cabo de Gata ranges, southeast Spain. *Geomorphology* 28, 1–22.
- Hillaire-Marcel, C.I., Gariépy, C., Ghalab, B., Goy, J.L., Zazo, C., Cuerda Barceló, J., 1996. U-series measurements in Tyrrhenian deposits from Mallorca. Further evidence for two Last-Interglacial high sea levels in the Balearic Islands. *Quaternary Science Reviews* 15, 53–62.



- Macklin, M.G., Fuller, I.C., Lewin, J., Maas, G.S., Passmore, D.G., Rose, J., Woodward, J.C., Black, S., Hamlin, R.H.B., Rowan, J.S., 2002. Correlation of fluvial sequences in the Mediterranean basin over the last 200 ka and their relationship to climate change. *Quaternary Science Reviews* 21, 1633–1641.
- Martín de la Cruz, J.C., Delgado, M.R., Sanz, M.P., Vera, J.C., 2000. Novedades en el conocimiento sobre el Neolítico y Calcolítico en Andalucía: panorámica de una década de investigaciones. *Trabajos de Arqueología* 16, 215–241.
- Martrat, B., Grimalt, J.O., López-Martínez, C., Cacho, I., Sierro, F.J., Flores, J.A., Zahn, R., Canals, M., Curtis, J.H., Hodell, D.A., 2004. Abrupt temperature changes in the Western Mediterranean over the last 250,000 years. *Science* 306, 1762–1765.
- McManus, J.F., Oppo, D.W., Cullen, J.L., 1999. A 0.5 million year record of millennial-scale climate variability in the North Atlantic. *Science* 283, 971–975.
- Menanteau, L., Vanney, J.R., Goy, J.L., Zazo, C., 1989. Mapa fisiográfico del litoral atlántico de Andalucía 1/50.000: M.F. 05: Cabo Roche-Ensenada de Bolonia. Junta de Andalucía (Ministerio de Medio Ambiente). Casa de Velázquez.
- Moreno, A., Cacho, I., Canals, M., Prins, M.A., Sánchez-Gómez, M.F., Grimalt, J.O., Weltje, G.J., 2002. Saharan dust transport and high latitude glacial climatic variability: the Alboran Sea record. *Quaternary Research* 58, 318–328.
- Muhs, D.R., Simmons, K.R., Steinke, B., 2002. Timing and warmth of the Last Interglacial period: new U-series evidence for Hawai and Bermuda and a new fossil compilation for North America. *Quaternary Science Reviews* 21, 1355–1383.
- Murray, A.S., Wintle, A.G., 2000. Luminescence dating of quartz using an improved single-aliquot regenerative-dose protocol. *Radiation Measurements* 32, 57–73.
- Prescott, J.R., Hutton, J.T., 1988. Cosmic ray and gamma ray dosimetry for TL and ESR. *Nuclear Tracks and Radiation Measurements* 14, 223–227.
- Reed, J.M., Stevenson, A.C., Juggins, S., 2001. A multi-proxy record of Holocene climatic change in southwestern Spain: the Laguna de Medina, Cadiz. *The Holocene* 11, 707–719.
- Sánchez-Gómez, M.F., Eynaud, F., Turon, J.L., Shackleton, N.J., 1999. High resolution palynological record off the Iberian margin: direct land-sea correlation for the last interglacial complex. *Earth and Planetary Science Letters* 171, 123–137.
- Sánchez-Gómez, M.F., Cacho, I., Turon, J.L., Guiot, J., Sierro, F.J., Peyrouquet, J.-P., Grimalt, J.O., Shackleton, N.J., 2002. Synchronicity between marine and terrestrial responses to millennial scale climatic variability during the last glacial period in the Mediterranean region. *Climate Dynamics* 19, 95–105.
- Sangode, S.J., Bloemendal, J., 2004. Pedogenic transformation of magnetic minerals in Pliocene–Pleistocene palaeosols of the Siwalik Group, NW Himalaya, India. *Palaeogeography, Palaeoclimatology, Palaeoecology* 212, 95–118.
- Sanz de Galdeano, C., López Garrido, A.C., 1991. Tectonic evolution of the Malaga Basin (Betic Cordillera). Regional implications. *Geodinamica Acta* 5, 173–186.
- Stoops, G., 2003. Guidelines for Analysis and Description of Soil and Regolith Thin Sections. Soil Science Society of America, Inc., Madison, Wisconsin, USA.
- U.S.D.A.-N.R.C.S., 2004. Soil Survey Laboratory Methods Manual. Soil Survey Inv. Rep. No 42.
- Yll, R., Zazo, C., Goy, J.L., Pérez-Obiol, R., Pantaleón-Cano, J., Civis, J., Dabrio, C.J., González, A., Borja, F., Soler, V., Lario, J., Luque, L., Sierro, F., González-Hernández, F.M., Lezine, A.M., Deneffe, M., Roure, J.M., 2003. Quaternary palaeoenvironmental changes in South Spain. In: Ruiz Zapata, B., Dorado, M., Valdeolmillos, A., Gil, M.J., Bardají, T., de Bustamante, I., Martínez Mendizábal, I., et al. (Eds.), *Quaternary Climatic Changes and Environmental Crises in the Mediterranean Region*. Servicio de Publicaciones, Universidad de Alcalá de Henares, España, pp. 201–213.
- Zazo, C., 1980. El Cuaternario marino-continental y el límite Plio-Pleistoceno en el litoral de Cádiz. PhD Thesis, Universidad Complutense de Madrid.
- Zazo, C., Goy, J.L., 1990. Hoja Vejer de la Frontera (n° 1073/1076). Plioceno superior y Cuaternario. Mapa Geológico de España 1:50.000 (2ª Serie). Instituto Tecnológico y Geominero de España.
- Zazo, C., Silva, P.G., Goy, J.L., Hillaire-Marcel, C., Ghaleb, B., Lario, J., Bardají, T., González, A., 1999. Coastal uplift in continental collision plate boundaries: data from the Last Interglacial marine terraces of the Gibraltar Strait area (south Spain). *Tectonophysics* 301, 95–109.
- Zazo, C., Goy, J.L., Dabrio, C.J., Bardají, T., Hillaire-Marcel, C., Ghaleb, B., González-Delgado, J.A., Soler, V., 2003. Pleistocene raised marine terraces of the Spanish Mediterranean and Atlantic coasts: records of coastal uplift, sea-level highstands and climate changes. *Marine Geology* 194, 103–133.
- Zazo, C., Mercier, N., Silva, P.G., Dabrio, C.J., Goy, J.L., Roquero, E., Soler, V., Borja, F., Lario, J., Polo, D., Luque, L., 2005. Landscape evolution and geodynamic controls in the Gulf of Cadiz (Huelva coast, SW Spain) during the Late Quaternary. *Geomorphology* 68, 269–290.